Multiagent System-Based Distributed Coordinated Control for Radial DC Microgrid Considering Transmission Time Delays

Dou, Chun-Xia; Yue, Dong; Guerrero, Josep M.; Xie, Xiangpeng; Hu, Songlin

Published in:
I E E E Transactions on Smart Grid

DOI (link to publication from Publisher):
10.1109/TSG.2016.2524688

Publication date:
2017

Document Version
Accepted author manuscript, peer reviewed version

Citation for published version (APA):
Dou, C-X., Yue, D., Guerrero, J. M., Xie, X., & Hu, S. (2017). Multiagent System-Based Distributed Coordinated Control for Radial DC Microgrid Considering Transmission Time Delays. *I E E E Transactions on Smart Grid*, *8*(5), 2370 - 2381 . https://doi.org/10.1109/TSG.2016.2524688

Multi-Agent-System based Distributed Coordinated Control for Radial DC Microgrid Considering Transmission Time Delays

Chunxia Dou , Dong Yue, *Senior, IEEE,* Josep M. Guerrero, *Fellow, IEEE,* Xiangpeng Xie, and Songlin Hu

***Abstract*—This paper focuses on a multi-agent based distributed coordinated control for radial DC microgrid considering transmission time delays. Firstly, a two-level multi-agent system is constructed, where local control is formulated based on local states and executed by means of the first-level agent, and distributed coordinated control law is formulated based on wide-area information and executed by means of the secondary-level agent in order to improve the voltage control performances. Afterwards, the research mainly focuses on designing the local controller and the distributed coordinated controller. For purpose of robust stability, the local control is designed as local state-feedback based H_∞ robust controller. It is worth mentioning that the distributed coordinated control consists of local state feedback control and decoupling coordinated control law that only come from adjacent DER units. Moreover, the distributed coordinated controller is designed by means of delay-dependent H_∞ robust control method taking into account transmission time delays. Finally, the validity of the proposed control scheme is demonstrated by means of simulation results.**

***Index terms*—DC microgrid, multi-agent-system, distributed coordinated control, time delay, robust control**

I. INTRODUCTION

THE increasing penetration of DC renewable energy sources and increasing use of DC loads have motivated a growing interest in DC microgrid (MG) [1], [2]. The DC network can integrate various kinds of small DC or non-60Hz frequency distributed energy resources (DERs) such as photovoltaic arrays, wind turbine and battery etc. to supply DC loads more efficiently. DC MGs have several advantages over their AC counterparts [3]. For instance, the control regarding reactive power and frequency is not an issue. So DC MGs have been widely regarded as one of the best means of using renewable energy resources to meet DC load demand.

The major concern in the stabilization operation problem of DC MGs is how to design a feasible and efficient control scheme to maintain bus voltage stabilization. In the last a few years, many researches considered the decentralized "peer to peer" control, which means that each DER subsystem is controlled independently based on its local available information, for example local droop control scheme [4]. This control mode is obviously feasible and efficient [5], [6]. However, the bus voltage of each DER subsystem usually changes with the DER operation state. Therefore, the decentralized "peer to peer" control scheme may lead to a large steady voltage deviation between two DER units. In order to solve this problem, many researchers proposed hierarchical coordinated strategies [7]-[9]. The secondary coordinated strategies are ordinarily divided into three types: the centralized communication and control scheme [10], centralized communication and decentralized control scheme [11] and distributed coordinated control scheme [12]-[17]. Due to huge dimensionality of MG and communication pressure, the first scheme is neither applicable nor economic. Although the second scheme implements secondary adjustment in a decentralized manner, but it still depends on global information, which leads to communication pressure and decreased reliability. On the contrary, as an effective means, the third scheme recently has attracted more attentions. In the distributed coordinated control scheme, a local controller of each DER unit at the first level is helped by a distributed coordinated controller at the secondary level. The secondary-level controller uses remote transmission signals that only come from the adjacent DER unit to synthesize decoupling control law in order to improve control performance. So this kind of scheme only depends on low bandwidth communication. However, In a MG, DERs are very dispersive and loosely connected to each other, so even two adjacent DERs are far away. When the control signals that come from adjacent DER unit are transmitted through the transmission line, communication delay is unavoidably introduced [18]. In general, the communication delay can vary from tens to several hundred milliseconds or more [18], [19]. The existence of time delays would deteriorate the control performance. Therefore, when designing the distributed coordinated control scheme, the time delay should be taken into consideration. The time delay stabilization problem can be classified into two types: delay-independent stabilization [20] and delay-dependent one [21].The delay-independent stabilization is considered more conservative in general than the delay-dependent one, especially for the system where time delay is actually small. Due to communication delays in MG are within the range of several hundred milliseconds [19], so the less conservative delay-dependent stabilization approach is more suitable for designing the distributed coordinated control scheme.

This work is supported by the National Natural Science Foundation of China under Grant 61573300, 61533010, 6140320 & 613040439.

C. Dou is with Institute of Advanced Technology, Nanjing University of Posts and Telecommunications, Nanjing, P. R. China, and with Institute of Electrical Engineering, Yanshan University, Qinhuangdao, P.R. China (e-mail: cxdou@ysu.edu.cn)

D. Yue (corresponding author), X. Xie and S. Hu are with Institute of Advanced Technology, Nanjing University of Posts and Telecommunications, Nanjing, P. R. China (e-mail: medongy@vip.163.com; xiexp@njupt.edu.cn; songlin621@126.com)

Josep M. Guerrero is with the Department of Energy Technology, Aalborg University, 9220 Aalborg East, Denmark (e-mail: joz@et.aau.dk)

Moreover, with respect to the two-level distributed coordinated scheme, the multi-agent system (MAS) technique is one of the best choices to make the control much intelligent and flexible [22]. MAS is composed of multiple agents, where each agent is not only autonomous and intelligent, but also interacts with each other in a cooperation manner, so that MAS is able to handle complex problems in a more flexible and intelligent way. So far, the researches regarding management and control of MGs had been done in multi-agent approach [23], [24]. In this paper, a two-level MAS based distributed coordinated control scheme is proposed, where each DER unit is associated with a unit control agent at the first level to deal with local control for its unit system, also where there is a distributed coordinated agent at the secondary level to implement the distributed coordinated control.

The research is decomposed into the following steps: (i) The MAS based distributed coordinated control scheme is constructed. Also the structures of two levels of agents are designed, respectively. (ii) According to the bus voltage deviation between any two adjacent DER units, the secondary-level agent determines what kind of control mode it needs to execute. (iii) Both local and distributed coordinated controllers in four kinds of control modes are designed. For purpose of robust stability, the local control is designed as local state-feedback based H_∞ robust controller. It is worth mentioning that, the distributed coordinated control consists of local state-feedback control and decoupling coordinated control law that only come from adjacent DER units, so that communication pressure is decreased largely. Moreover, for improving control performance, the distributed coordinated control is designed by means of delay-dependent H_∞ robust control method taking into account the communication time delays. The sufficient conditions for controller existence in four kinds of control modes are transformed into line matrix inequality (LMI) convex optimization problem. (iv) The validity of the proposed control scheme is demonstrated by means of simulation study.

II. The MAS Based Distributed Coordinated Control Scheme of DC MG

The proposed MAS based distributed coordinated control scheme for radial DC MG is depicted in Fig.1. The radial DC MG contains multiple DER units connected with each other in proper order through a DC line. And each DER unit supplies a local load connected on the point of common coupling (PCC) node. Here, a hierarchical MAS that consists of first-level unit control agents and secondary-level distributed coordinated control agents, is proposed to implement distributed coordinated control for the radial DC MG.

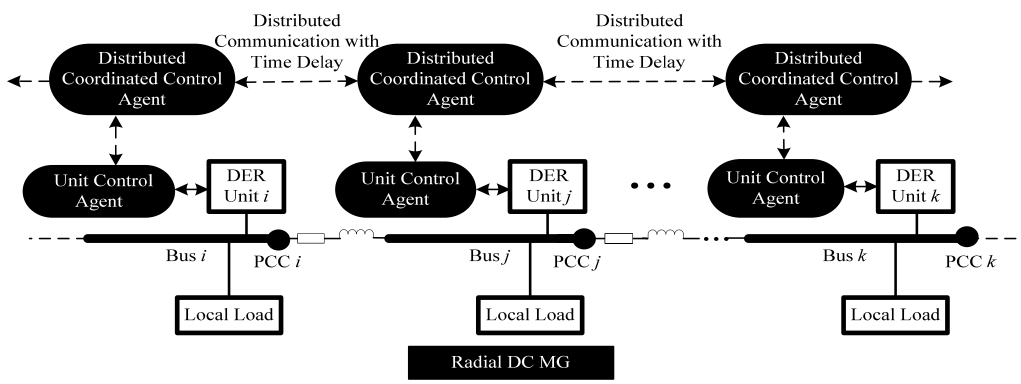

Fig.1 MAS based distributed coordinated control scheme

Corresponding to Fig.1, each first-level unit control agent is mainly responsible for formulating and implementing the local control for its DER unit. It is designed as hybrid agent, which is composed of reactive layer and deliberative layer as shown in Fig.2. The reactive layer is defined as "recognition, perception and action" and has priority to respond quickly to emergencies of environment. The deliberative layer is defined as "belief, desire and intention", and has high intelligence to control the dynamic behavior of its DER unit.

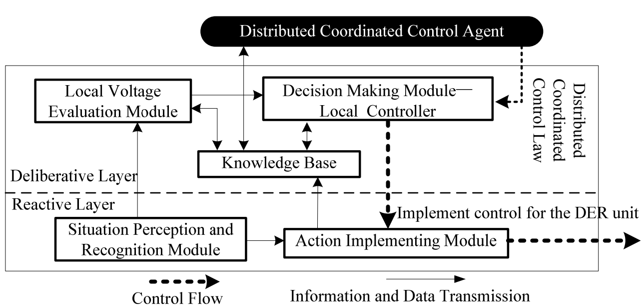

Fig.2 Structure of the first-level unit control agent

Each secondary-level distributed coordinated control agent is mainly responsible determining what kind of control mode and implementing the distribution coordinated control law for its DER unit to improve control performance. The distributed coordinated control law is formulated by using wide-area states that only come from the adjacent DER unit. Each secondary-level agent is designed as a deliberative agent. The voltage deviation between any two adjacent DER units is estimated in voltage assessment module. The distributed coordinated control law is formulated in decision-making module. When the voltage deviation is larger than a specified threshed, the distributed coordinated control law is executed through action implementation module.

In the hierarchical MAS, the interactive manner among agents divides into two categories [25]: no fixed master-slave mode and master-slave mode. For example, when the request of one unit agent is responded by another unit agent, this kind of interaction is no fixed master-slave mode. While when the distributed coordinated control agent requests to send the coordinated control law to the unit agent, the request must be responded by the unit agent, in this case this kind of interaction is master-slave mode. The request of the coordinated control agent has the higher priority than that of any unit agent.

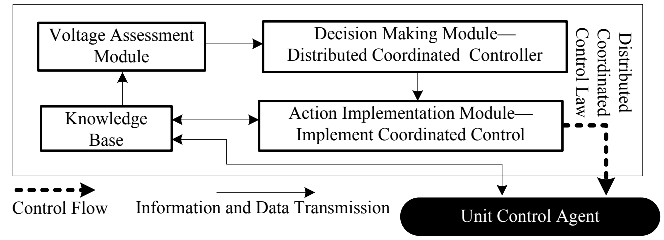

Fig.3 Structure of the secondary-level distributed coordinated control agent

III. Control Mode and Dynamic Modeling

Corresponding to Fig.1, the dynamic model of any three adjacent DER units is built as shown in Fig.4. In Fig.4, the *p*th DER is connected among both *q*th and *r*th DERs through DC lines with different impedances specified by parameters $R_{pq}=R_{qp}>0$, $L_{pq}>0$, $R_{pr}=R_{rp}>0$ and $L_{pr}>0$. In each DER unit, a Buck converter is presented to supply a local DC load connected to the PCC through a LC filter. The local load is unknown and is treated as current disturbance.

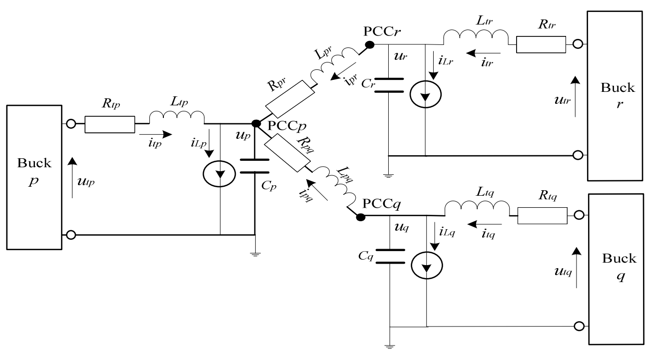

Fig.4 Dynamic model of three adjacent DER units

Corresponding to Fig.4, according to Kirchoff's voltage law and Kirchoff's current law, the following set of equations is obtained

$$\text{DER } p\begin{cases}\dfrac{du_p}{dt}=\dfrac{1}{C_i}i_{tp}-\dfrac{1}{C_i}i_{Lp}+\dfrac{1}{C_i}(i_{pq}+i_{pr})\\[2mm] \dfrac{di_{tp}}{dt}=-\dfrac{1}{L_{tp}}u_p-\dfrac{R_{tp}}{L_{tp}}i_{tp}+\dfrac{1}{L_{tp}}u_{tp}\end{cases}\tag{1}$$

$$\text{DER } k\in\{q,r\}\begin{cases}\dfrac{du_k}{dt}=\dfrac{1}{C_k}i_{tk}-\dfrac{1}{C_k}i_{Lk}+\dfrac{1}{C_k}i_{kp}\\[2mm] \dfrac{di_{tk}}{dt}=-\dfrac{1}{L_{tk}}u_k-\dfrac{R_{tk}}{L_{tk}}i_{tk}+\dfrac{1}{L_{tk}}u_{tk}\end{cases}\tag{2}$$

As [25], since i_{pq} and i_{pr} are currents on DC transmission line, $di_{pq}/dt=-di_{qp}/dt=0$ and $di_{pr}/dt=-di_{qr}/dt=0$. Therefore, the following equations are given

$$i_{pq}=-i_{qp}=(u_q-u_p)/R_{pq}\tag{3}$$

$$i_{pr}=-i_{rp}=(u_r-u_p)/R_{pr}\tag{4}$$

Remark 3.1: According to Eqs. (3) and (4), when $|u_q-u_p|\le\varepsilon_{pq}$ and $|u_r-u_p|\le\varepsilon_{pr}$, where ε_{pq} and ε_{pr} are small specified thresholds, $|i_{pq}|$ and $|i_{pr}|$ are very small, since R_{pq} and R_{pr} are constant. In this case, $i_{pq}+i_{pr}$, i_{pq} and i_{pr} are regarded as current disturbances, then the three DER units can be described as follows

$$\text{DER}i:\ \dot{\boldsymbol{x}}_i(t)=\boldsymbol{A}_i\boldsymbol{x}_i(t)+\boldsymbol{B}_iv_i(t)+\boldsymbol{D}_i\boldsymbol{\omega}_i(t),\ i\in\{p,q,r\}\tag{5}$$

where $\boldsymbol{x}_i(t)=[u_i(t),i_{ti}(t)]^{\mathrm{T}}$ is state vectors; $v_i(t)=u_{ti}(t)$ is input variables; $\boldsymbol{\omega}_p(t)=[i_{Lp}(t),(i_{pq}(t)+i_{pr}(t))]^T$, $\boldsymbol{\omega}_q(t)=[i_{Lq}(t),\ i_{qp}(t)]^T$ and $\boldsymbol{\omega}_r(t)=[i_{Lr}(t),\ i_{rp}(t)]^T$ are disturbance vectors of the three DER units, respectively; the coefficient matrices are as follows

$$\boldsymbol{A}_i=\begin{bmatrix}0 & 1/C_i\\ -1/L_{ti} & -R_{ti}/L_{ti}\end{bmatrix};\ \boldsymbol{B}_i=\begin{bmatrix}0\\ 1/L_{ti}\end{bmatrix};\ \boldsymbol{D}_i=\begin{bmatrix}-1/C_i & 1/C_i\\ 0 & 0\end{bmatrix}.$$

Since there is not coupling in Eq.(5), the three DER units can be respectively controlled only by means of their own local controller in the first-level unit agent. The local controller design will be discussed in Section IV. A. According to Remark 3.1, the control mode of the three DER units is defined as control mode 1.

Remark 3.2: When $|u_q-u_p|>\varepsilon_{pq}$ and $|u_r-u_p|\le\varepsilon_{pr}$, $|i_{pq}|$ is no longer very small, thus $i_{pq}+i_{pr}$ and i_{pq} are also no longer deemed as current disturbances. In this case, taking into account transmission time delay, both *p*th and *q*th DER units are described in the following form

$$\text{DER}i:\ \dot{\boldsymbol{x}}_i(t)=\widetilde{\boldsymbol{A}}_{ij}\boldsymbol{x}_i(t)+\boldsymbol{B}_iv_i(t)+\boldsymbol{A}_{ij}\boldsymbol{x}_j(t-\tau_{ij})+\widetilde{\boldsymbol{D}}_i\boldsymbol{\omega}_i(t)\tag{6}$$

where $i\in\{p,q\},\ j\in\{p,q\},i\ne j$; $\tau_{pq}=\tau_{qp}\le\bar{\tau},\ (\bar{\tau}>0)$ is the transmission time delay between *p*th DER and *q*th DER, $\boldsymbol{x}_j(t-\tau_{ij})=[u_j(t-\tau_{ij}),i_{tj}(t-\tau_{ij})]^{\mathrm{T}}$, $\boldsymbol{B}_i$ is in the same form of Eq.(5),

$$\widetilde{\boldsymbol{A}}_{ij}=\begin{bmatrix}-1/R_{ij}C_i & 1/C_i\\ -1/L_{ti} & -R_{ti}/L_{ti}\end{bmatrix},\ \boldsymbol{A}_{ij}=\begin{bmatrix}1/R_{ij}C_i & 0\\ 0 & 0\end{bmatrix},\ \widetilde{\boldsymbol{D}}_i=\begin{bmatrix}-1/C_i & 0\\ 0 & 0\end{bmatrix}.$$

In Eq.(6), since there is coupling between *p*th DER and *q*th DER, the two DER units need to be controlled by means of the local controller combined with the decoupling coordinated control law. The MAS based delay-dependent distributed coordinated controller will be studied in Section IV. B. While the *r*th DER units is still described in the same form of Eq.(5), where only $i=r$. Therefore, the *r*th DER unit can be controlled only by means of the local controller in the first-level unit agent. According to Remark 3.2, the control mode of the three DER units is defined as control mode 2.

Remark 3.3: When $|u_r-u_p|>\varepsilon_{pr}$ and $|u_q-u_p|\le\varepsilon_{pq}$, for the same reason, both *p*th and *k*th DER units are described in a similar form of Eq.(6), where only $i\in\{p,r\},\ j\in\{p,r\},i\ne j$, $\tau_{pr}=\tau_{rp}\le\bar{\tau},\ (\bar{\tau}>0)$ is the transmission time delay between the *p*th DER and the *r*th DER. In this case, the two DER units need to be controlled by means of the MAS based delay-dependent distributed coordinated controller. While the *q*th DER units can be described in the same form of Eq.(5) ,where only $i=q$. Therefore, the *q*th DER unit can be controlled only by means of the local controller in the first-level unit agent. According to Remark 3.3, the control mode of the three DER units is defined as control mode 3.

Remark 3.4: When $|u_q-u_p|>\varepsilon_{pq}$ and $|u_r-u_p|>\varepsilon_{pr}$, all currents including $i_{pq}+i_{pr}$, i_{pq} and i_{pr} are no longer dealt as current disturbances. In this case, both *q*th and *k*th DER units are described in a similar form of Eq.(6) where only $i \in \{q,k\}$, $j = p$. While the pth DER unit is described as

$$\text{DER}p\text{: } \dot{\boldsymbol{x}}_p(t) = \widetilde{\boldsymbol{A}}_{pqr}\boldsymbol{x}_p(t) + \boldsymbol{B}_p v_p(t) + \boldsymbol{A}_{pq}\boldsymbol{x}_q(t-\tau_{pq}) + \boldsymbol{A}_{pr}\boldsymbol{x}_r(t-\tau_{pr}) + \widetilde{\boldsymbol{D}}_p\boldsymbol{\omega}_p(t) \tag{7}$$

where, $\widetilde{\boldsymbol{A}}_{pqr} = \begin{bmatrix} -1/R_{pq}C_p - 1/R_{pr}C_p & 1/C_p \\ -1/L_{tp} & -R_{tp}/L_{tp} \end{bmatrix}$, other coefficient matrices are in a similar form of Eq.(6) only $i = p$, $j \in \{q,r\}$.

The three DER units need to be controlled by means of the MAS based delay-dependent distributed coordinated controller. According to Remark 3.4, the control mode of the three DER units is defined as control mode 4.

No matter the local controller or the distributed coordinated controller, their control goal is to guarantee the state variables (voltage and current) to track their reference values. Therefore, here, the tracking reference model is given for the pth, qth and rth DER units as follows

$$\dot{\boldsymbol{x}}_{ri}(t) = \boldsymbol{A}_{ri}\boldsymbol{x}_{ri}(t) + \boldsymbol{r}_i(t),\ i \in \{p,q,r\} \tag{8}$$

where $\boldsymbol{x}_{ri}(t)$ represents a desired trajectory for $\boldsymbol{x}_i(t)$ to follow. $\boldsymbol{A}_{ri}$ is a specific asymptotically stable matrix, and $\boldsymbol{r}_i(t)$ denotes bounded reference input.

IV. The Controller Design

A. Local Controller Design in First-level Unit Agent

When one DER unit (including each DER unit in remark 3.1, the rth DER unit in remark 3.2, and the qth DER unit in remark 3.3) is modeled in the form of Eq.(5), it can be controlled by means of only local controller in the first-level unit control agent. The local controller is designed as

$$v_i(t) = \boldsymbol{K}_i[\boldsymbol{x}_i(t) - \boldsymbol{x}_{ri}(t)],\ i \in \{p,q,r\} \tag{9}$$

where $\boldsymbol{K}_i$ is local controller parameter matrix of ith DER unit. Then, by using Eq (5) and Eq.(8), the ith DER tracking control system under the local controller (9) is written in the following form

$$\text{DER}i: \dot{\hat{\boldsymbol{x}}}_i(t) = \hat{\boldsymbol{A}}_i\hat{\boldsymbol{x}}_i(t) + \hat{\boldsymbol{D}}_i\hat{\boldsymbol{\omega}}_i(t) \tag{10}$$

where, $\hat{\boldsymbol{x}}_i(t) = \left[\boldsymbol{x}_i^T(t),\ \boldsymbol{x}_{ri}^T(t)\right]^T$, $\hat{\boldsymbol{\omega}}_i(t) = \left[\boldsymbol{\omega}_i^T(t),\ \boldsymbol{r}_i^T(t)\right]^T$, and

$$\hat{\boldsymbol{A}}_i = \begin{bmatrix} \boldsymbol{A}_i + \boldsymbol{B}_i\boldsymbol{K}_i & -\boldsymbol{B}_i\boldsymbol{K}_i \\ 0 & \boldsymbol{A}_{ri} \end{bmatrix},\ \hat{\boldsymbol{D}}_i = \begin{bmatrix} \boldsymbol{D}_i & 0 \\ 0 & \boldsymbol{I} \end{bmatrix}.$$

H_∞ control performance regarding the tracking error is given in the following form

$$\frac{\int_0^{t_f}[(\boldsymbol{x}_i(t) - \boldsymbol{x}_{ri}(t))^T\boldsymbol{Q}_i(\boldsymbol{x}_i(t) - \boldsymbol{x}_{ri}(t))]dt}{\int_0^{t_f}\hat{\boldsymbol{\omega}}_i(t)^T\hat{\boldsymbol{\omega}}_i(t)dt} \le \rho_i^2 \tag{11}$$

where t_f denotes terminal time of control, and the weighting matrix $\boldsymbol{Q}_i = \boldsymbol{Q}_i^T > 0$. Physical meaning of (11) is that effect of any $\hat{\omega}_i(t)$ on tracking error $\boldsymbol{x}_i(t) - \boldsymbol{x}_{ri}(t)$ must be attenuated below a desire level ρ_i from viewpoint of energy. H_∞ control performance with a prescribed attenuation level is useful for a robust control design without knowledge of $\boldsymbol{\omega}_i(t)$ and $\boldsymbol{r}_i(t)$.

Considering the initial condition, H_∞ control performance can be rewritten as follows:

$$\int_0^{t_f}\hat{\boldsymbol{x}}_i^T(t)\hat{\boldsymbol{Q}}_i\hat{\boldsymbol{x}}_i(t)dt \le \rho_i^2\int_0^{t_f}\hat{\boldsymbol{\omega}}_i^T(t)\hat{\boldsymbol{\omega}}_i(t)dt + \hat{\boldsymbol{x}}_i^T(0)\boldsymbol{P}_i\hat{\boldsymbol{x}}_i(0) \tag{12}$$

where $\hat{\boldsymbol{Q}}_i = \begin{bmatrix} \boldsymbol{Q}_i & -\boldsymbol{Q}_i \\ -\boldsymbol{Q}_i & \boldsymbol{Q}_i \end{bmatrix}$, and weighting matrix $\boldsymbol{P}_i = \boldsymbol{P}_i^T > 0$.

According to the following Theorem 4.1, the first-level unit control agent can determine the local controller (9) for the ith tracking system (10) with the guaranteed H_∞ control performance (12) for $\forall\hat{\boldsymbol{\omega}}_i(t)$.

Theorem 4.1 The ith DER unit tracking control system (10) is asymptotically stable with the guaranteed H_∞ control performance in (12) for $\forall\hat{\boldsymbol{\omega}}_i(t)$ if there exists $\boldsymbol{P}_i = \boldsymbol{P}_i^T > 0$, satisfying the following matrix inequality

$$\begin{bmatrix} \hat{\boldsymbol{A}}_i^T\boldsymbol{P}_i + \boldsymbol{P}_i\hat{\boldsymbol{A}}_i + \hat{\boldsymbol{Q}}_i & \boldsymbol{P}_i\hat{\boldsymbol{D}}_i \\ \hat{\boldsymbol{D}}_i^T\boldsymbol{P}_i & -\rho_i^2\boldsymbol{I} \end{bmatrix} \le 0. \tag{13}$$

The proof is given in Appendix A

The inequality (13) can be transformed into linear matrix inequality (LMI) according to the following procedures

(1) Denote a new matrix

$$\boldsymbol{W}_i = \begin{bmatrix} \overline{\boldsymbol{W}}_i & 0 \\ 0 & \boldsymbol{I} \end{bmatrix} = \begin{bmatrix} \boldsymbol{P}_i^{-1} & 0 \\ 0 & \boldsymbol{I} \end{bmatrix}$$

where $\overline{\boldsymbol{W}}_i^T = \overline{\boldsymbol{W}}_i = \boldsymbol{P}_i^{-1} > 0$, left and right multiplying it into (14), it can be obtained

$$\begin{bmatrix} \overline{\boldsymbol{W}}_i\hat{\boldsymbol{A}}_i^T + \hat{\boldsymbol{A}}_i\overline{\boldsymbol{W}}_i + \overline{\boldsymbol{W}}_i\hat{\boldsymbol{Q}}_i\overline{\boldsymbol{W}}_i & \hat{\boldsymbol{D}}_i \\ \hat{\boldsymbol{D}}_i^T & -\rho_i^2\boldsymbol{I} \end{bmatrix} \le 0 \tag{14}$$

(2) Define

$$\overline{\boldsymbol{W}}_i = \begin{bmatrix} \overline{\boldsymbol{W}}_{i1} & 0 \\ 0 & \overline{\boldsymbol{W}}_{i1} \end{bmatrix} = \begin{bmatrix} \boldsymbol{P}_{i1}^{-1} & 0 \\ 0 & \boldsymbol{P}_{i1}^{-1} \end{bmatrix},\ \hat{\boldsymbol{K}}_i = \boldsymbol{K}_i\overline{\boldsymbol{W}}_{i1},\ \breve{\boldsymbol{Q}} = \overline{\boldsymbol{W}}_1\boldsymbol{Q}\overline{\boldsymbol{W}}_1,$$

it is easy to gain

$$\hat{\boldsymbol{A}}_i\overline{\boldsymbol{W}}_1 = \begin{bmatrix} \boldsymbol{A}_i\overline{\boldsymbol{W}}_{i1} + \boldsymbol{B}_i\hat{\boldsymbol{K}}_i & -\boldsymbol{B}_i\hat{\boldsymbol{K}}_i \\ 0 & \boldsymbol{A}_{ri}\overline{\boldsymbol{W}}_{i1} \end{bmatrix}.$$

Hence, the inequality (14) is equivalent to LMI.

Remark 4.1 The local controller design in (9) is transformed into the following LMI convex optimization problem

$$\min_{\overline{\boldsymbol{W}}_i,\ \hat{\boldsymbol{K}}_i} \rho_i^2,$$

$$\text{subject to } \overline{\boldsymbol{W}}_i = \overline{\boldsymbol{W}}_i^T > 0 \text{ and (14).} \tag{15}$$

B. MAS based Distributed Coordinated Controller Design

1. Distributed coordinated controller design between two DER units

When two DER units (including both pth and qth DER units in remark 3.2, as well as both pth and rth DER units in remark 3.3) are modeled in the form of Eq.(6), they need to be controlled by means of the two-level MAS. The distributed coordinated controller is designed as

$$v_i(t) = \boldsymbol{K}_i[\boldsymbol{x}_i(t) - \boldsymbol{x}_{ri}(t)] + \boldsymbol{K}_{ij}\boldsymbol{x}_j(t-\tau_{ij}) \tag{16}$$

where $i \in \{p,q\}, j \in \{p,q\}, i \ne j$; or $i \in \{p,r\}, j \in \{p,r\}, i \ne j$; $\boldsymbol{K}_i$ is local controller parameter matrix of the ith DER unit, $\boldsymbol{K}_{ij}$ is decoupling coordinated control law that comes form jth DER unit.

By Eqs (6) and (8), the ith tracking control system under the controller (16) is given as follows

$$\text{DER}i\text{: } \dot{\hat{\boldsymbol{x}}}_i(t) = \overline{\boldsymbol{A}}_{ij}\hat{\boldsymbol{x}}_i(t) + \overline{\boldsymbol{A}}_{ij}\hat{\boldsymbol{x}}_j(t-\tau_{ij}) + \overline{\boldsymbol{D}}_i\hat{\boldsymbol{\omega}}_i(t) \tag{17}$$

where $i \in \{p,q\}, j \in \{p,q\}, i \ne j$; or $i \in \{p,r\}, j \in \{p,r\}, i \ne j$,

$$\overline{A}_{ij}=\begin{bmatrix}\widetilde{A}_{ij}+B_iK_i & -B_iK_i\\ 0 & A_{ri}\end{bmatrix},\overline{A}_{ij}=\begin{bmatrix}A_{ij}+B_iK_{ij} & 0\\ 0 & 0\end{bmatrix},\overline{D}_i=\begin{bmatrix}\widetilde{D}_i & 0\\ 0 & I\end{bmatrix}.$$

Then augmented system by integrating the *i*th DER with the *j*th DER is described as

$$\text{DER}ij:\ \dot{\widetilde{x}}(t)=\widetilde{A}\widetilde{x}(t)+\widehat{A}\widetilde{x}(t-\tau_{ij})+\widetilde{D}\widetilde{\omega}(t) \tag{18}$$

where $i=p,\ j\in\{q,r\}$; $\widetilde{x}(t)=\left[x_i^T(t),x_{ri}^T(t),x_j^T(t),x_{rj}^T(t)\right]^{\mathrm{T}}$ is the state vector of the augmented system, $\widetilde{v}(t)=\left[v_i(t),v_j(t)\right]^{\mathrm{T}}$ is the input vector and $\widetilde{\omega}(t)=\left[\omega_i^T(t),\ \omega_j^T(t)\right]^T$ is the disturbance vector of the augmented system. Moreover,

$$\widetilde{A}=\begin{bmatrix}\overline{A}_{ij} & 0\\ 0 & \overline{A}_{ji}\end{bmatrix},\widehat{A}=\begin{bmatrix}0 & \overline{A}_{ij}\\ \overline{A}_{ji} & 0\end{bmatrix},\widetilde{D}=\begin{bmatrix}\overline{D}_i & 0\\ 0 & \overline{D}_j\end{bmatrix}.$$

Corresponding to the augmented system (18), H_∞ control performance can be given as follows:

$$\int_0^{t_f}\widetilde{x}^T(t)\widetilde{Q}\widetilde{x}(t)dt\le\rho^2\int_0^{t_f}\widetilde{\omega}^T(t)\widetilde{\omega}(t)dt+\mathrm{V}(0) \tag{19}$$

where $\widetilde{Q}=\begin{bmatrix}Q_i & -Q_i & 0 & 0\\ -Q_i & Q_i & 0 & 0\\ 0 & 0 & Q_j & -Q_j\\ 0 & 0 & -Q_j & Q_j\end{bmatrix}$, V(0) is Lyapunov function initial value.

By mans of the following Theorem 4. 2, the two-level agents can determine the distributed coordinated controller (16) for the augmented system (18) with the guaranteed H_∞ control performance (19) for $\forall\widetilde{\omega}(t)$.

Theorem 4.2 Given allowable upper bound $\overline{\tau}$ of the time delays, the controlled system (18) is asymptotically stable for all time-delays satisfying $\tau_{ij}\in[0,\overline{\tau}]$ with the H_∞ control performance in (19), if there exist symmetric positive definite matrices P , S , Z , X satisfying the following matrix inequalities

$$\begin{bmatrix}\Theta & P\widehat{A}-Y & P\widetilde{D} & \overline{\tau}\widetilde{A}^TZ\\ * & -S & 0 & \overline{\tau}\widehat{A}^TZ\\ * & * & -\rho^2 & \overline{\tau}\widetilde{D}^TZ\\ * & * & * & -\overline{\tau}Z\end{bmatrix}\le 0 \tag{20}$$

and $\begin{bmatrix}X & Y\\ Y^T & Z\end{bmatrix}\ge 0$.

where, $i=p,\ j\in\{q,r\}$, $\Theta=\widetilde{Q}+S+P\widetilde{A}+\widetilde{A}^TP+\overline{\tau}X+Y+Y^T$.

The proof is given in the Appendix B.

The inequality (20) is not linear, so left multiply and right multiply matrix $diag\{P^{-1},I,I,Z^{-1}\}$, then define

$$P^{-1}=\begin{bmatrix}P_1^{-1} & 0 & 0 & 0\\ 0 & P_1^{-1} & 0 & 0\\ 0 & 0 & P_1^{-1} & 0\\ 0 & 0 & 0 & P_1^{-1}\end{bmatrix},P_1=P_1^T>0,$$

$\widetilde{K}_i=K_iP_1^{-1}$, $\widetilde{K}_j=K_jP_1^{-1}$, $\widetilde{K}_{ij}=K_{ij}P_1^{-1}$, $\widetilde{K}_{ji}=K_{ji}P_1^{-1}$, $\widetilde{X}=P^{-1}XP^{-1}$, $\widetilde{S}=P^{-1}SP^{-1}$, $\widehat{Q}=P^{-1}\widetilde{Q}P^{-1}$, $\widetilde{Y}=P^{-1}YP^{-1}$,

it is easy to gain,

$$\widetilde{A}P^{-1}=\begin{bmatrix}\widetilde{A}_{ij}P_1^{-1}+B_i\widetilde{K}_i & -B_i\widetilde{K}_i & 0 & 0\\ 0 & A_{ri}P_1^{-1} & 0 & 0\\ 0 & 0 & \widetilde{A}_{ji}P_1^{-1}+B_j\widetilde{K}_j & -B_j\widetilde{K}_j\\ 0 & 0 & 0 & A_{rj}P_1^{-1}\end{bmatrix}.$$

Then the inequality (20) is transformed to LMI (21).

$$\begin{bmatrix}\widetilde{\Theta} & \widehat{A}-P^{-1}Y & \widetilde{D} & \overline{\tau}P^{-1}\widetilde{A}^T\\ * & -S & 0 & \overline{\tau}\widehat{A}^T\\ * & * & -\rho^2 & \overline{\tau}\widetilde{D}^T\\ * & * & * & -\overline{\tau}Z^{-1}\end{bmatrix}\le 0 \tag{21}$$

where $\widetilde{\Theta}=\widehat{Q}+\widetilde{S}+\widetilde{A}P^{-1}+P^{-1}\widetilde{A}^T+\overline{\tau}\widetilde{X}+\widetilde{Y}+\widetilde{Y}^T$.

Remark 4.2 The distributed coordinated controller design in (16) is transformed into the following LMI convex optimization problem

$$\min_{P^{-1},\widetilde{K}_i,\widetilde{K}_j,\widetilde{K}_{ij},\widetilde{K}_{ji}}\rho^2,$$

$$\text{subject to } P^{-1}=P^{-T}>0,\ \begin{bmatrix}X & Y\\ Y^T & Z\end{bmatrix}\ge 0,\text{ and (21)} \tag{22}$$

where $i=p,\ j\in\{q,r\}$.

2. Distributed coordinated controller design among three DER units

When three DER units are described as remark 3.4, the two-level MAS needs to implement the distributed coordinated control among three DER units. In this case, the distributed coordinated controller is designed as

$$v_i(t)=K_i[x_i(t)-x_{ri}(t)]+K_{ij}x_j(t-\tau_{ij}),\ \ i\in\{q,r\},\ j=p \tag{23}$$

$$v_p(t)=K_p[x_p(t)-x_{rp}(t)]+K_{pq}x_q(t-\tau_{pq})+K_{pr}x_r(t-\tau_{pr}) \tag{24}$$

where the definition regarding controller parameters is similar to Eq.(16).

By Eqs (6) and (8), the *i*th tracking control system under the controller (23) is given as follows

$$\text{DER}i:\ \dot{\hat{x}}_i(t)=\overline{A}_{ij}\hat{x}_i(t)+\overline{A}_{ij}\hat{x}_j(t-\tau_{ij})+\overline{D}_i\hat{\omega}_i(t),\ i\in\{q,r\},\ j=p \tag{25}$$

where the coefficient matrices are in a similar form of Eq.(17), only $i\in\{q,r\},\ j=p$.

By Eqs (7) and (8), the *p*th tracking control system under the controller (24) is given as follows

$$\text{DER}p:\ \dot{\hat{x}}_p(t)=\overline{A}_{pqr}\hat{x}_i(t)+\overline{A}_{pq}\hat{x}_q(t-\tau_{pq})+\overline{A}_{pr}\hat{x}_r(t-\tau_{pr})+\overline{D}_p\hat{\omega}_p(t) \tag{26}$$

where $\overline{A}_{pqr}=\begin{bmatrix}\widetilde{A}_{pqr}+B_pK_p & -B_pK_p\\ 0 & A_{rp}\end{bmatrix}$, other coefficient matrices are in a similar form of Eq.(17) only $i=p,\ j\in\{q,r\}$.

Then augmented system by integrating the three DER units is described as

$$\text{DER}pqr:\ \dot{\widetilde{x}}(t)=\widetilde{A}_1\widetilde{x}(t)+\widehat{A}_1\widetilde{x}(t-\tau)+\widetilde{D}_1\widetilde{\omega}(t) \tag{27}$$

where $\widetilde{x}(t)=\left[x_p^T(t),x_{rp}^T(t),x_q^T(t),x_{rq}^T(t),x_r^T(t),x_{rr}^T(t)\right]^{\mathrm{T}}$ is the state vector, $\widetilde{x}(t-\tau)=\left[x_p^T(t),x_{rp}^T(t),x_q^T(t-\tau_{pq}),x_{rq}^T(t),x_r^T(t-\tau_{pr}),x_{rr}^T(t)\right]^{\mathrm{T}}$ $\widetilde{v}(t)=\left[v_p(t),v_q(t),v_r(t)\right]^{\mathrm{T}}$ is the input vector of the augmented system, and $\widetilde{\omega}(t)=\left[\omega_p^T(t),\ \omega_q^T(t),\ \omega_r^T(t)\right]^T$ is the disturbance vector. Moreover,

$$\widetilde{A}_1=\begin{bmatrix}\overline{A}_{pqr} & 0 & 0\\ 0 & \overline{A}_{qp} & 0\\ 0 & 0 & \overline{A}_{rp}\end{bmatrix},\ \widehat{A}_1=\begin{bmatrix}0 & \overline{A}_{pq} & \overline{A}_{pr}\\ \overline{A}_{qp} & 0 & 0\\ \overline{A}_{rp} & 0 & 0\end{bmatrix},\ \widetilde{D}_1=\begin{bmatrix}\overline{D}_p & 0 & 0\\ 0 & \overline{D}_q & 0\\ 0 & 0 & \overline{D}_r\end{bmatrix}.$$

Remark 4.3 According to the similar design process of Theorem 4.2, the distributed coordinated controller design in (23) and (24) is transformed into the following LMI convex optimization problem

$$\min_{P^{-1},\widetilde{K}_p,\widetilde{K}_q,\widetilde{K}_r,\widetilde{K}_{pq},\widetilde{K}_{qp},\widetilde{K}_{pr},\widetilde{K}_{rp}}\rho^2,$$

subject to $\boldsymbol{P}^{-1}=\begin{bmatrix}\boldsymbol{P}_1^{-1} & 0 & \cdots & 0\\ 0 & \boldsymbol{P}_1^{-1} & \cdots & 0\\ \vdots & \vdots & \ddots & \vdots\\ 0 & 0 & \cdots & \boldsymbol{P}_1^{-1}\end{bmatrix}^{6\times 6}$, $\boldsymbol{P}_1=\boldsymbol{P}_1^T>0$,

$$\begin{bmatrix}\boldsymbol{X} & \boldsymbol{Y}\\ \boldsymbol{Y}^T & \boldsymbol{Z}\end{bmatrix}\geq 0,\ \text{and}\ \begin{bmatrix}\widetilde{\Theta}_1 & \widehat{\boldsymbol{A}}_1-\boldsymbol{P}^{-1}\boldsymbol{Y} & \widetilde{\boldsymbol{D}}_1 & \bar{\tau}\boldsymbol{P}^{-1}\widetilde{\boldsymbol{A}}_1^T\\ * & -\boldsymbol{S} & 0 & \bar{\tau}\widehat{\boldsymbol{A}}_1^T\\ * & * & -\rho^2 & \bar{\tau}\widetilde{\boldsymbol{D}}_1^T\\ * & * & * & -\bar{\tau}\boldsymbol{Z}^{-1}\end{bmatrix}\leq 0\ . \quad (22)$$

where $\widehat{\boldsymbol{Q}}_1=\boldsymbol{P}^{-1}\begin{bmatrix}\hat{\boldsymbol{Q}}_p & 0 & 0\\ 0 & \hat{\boldsymbol{Q}}_q & 0\\ 0 & 0 & \hat{\boldsymbol{Q}}_r\end{bmatrix}$, $\hat{\boldsymbol{Q}}_i=\begin{bmatrix}\boldsymbol{Q}_i & -\boldsymbol{Q}_i\\ -\boldsymbol{Q}_i & \boldsymbol{Q}_i\end{bmatrix}$, $i\in\{p,q,r\}$, $\widetilde{\Theta}_1=\widehat{\boldsymbol{Q}}_1+\widetilde{\boldsymbol{S}}+\widetilde{\boldsymbol{A}}_1\boldsymbol{P}^{-1}+\boldsymbol{P}^{-1}\widetilde{\boldsymbol{A}}_1^T+\bar{\tau}\widetilde{\boldsymbol{X}}+\widetilde{\boldsymbol{Y}}+\widetilde{\boldsymbol{Y}}^T$, the definition regarding $\widetilde{\boldsymbol{K}}_p,\widetilde{\boldsymbol{K}}_q,\widetilde{\boldsymbol{K}}_r,\widetilde{\boldsymbol{K}}_{pq},\widetilde{\boldsymbol{K}}_{pr},\widetilde{\boldsymbol{K}}_{qp},\widetilde{\boldsymbol{K}}_{rp},\widetilde{\boldsymbol{S}},\widetilde{\boldsymbol{X}},\widetilde{\boldsymbol{Y}}$ is similar to remark 4.2.

C. Implementation of the Distributed Coordinated Control

The *p*th DER unit in DC MG can be controlled in four kinds of modes. The first mode is that the DER unit is controlled only by the local controller in the first-level unit agent. The second mode is that the DER unit is controlled by the distributed coordinated controller between both *p*th and *q*th DERs based on MAS. The third mode is by the distributed coordinated controller between both *p*th and *r*th DERs. The fourth mode is by the distributed coordinated controller among the *p*th, *q*th and *r*th DERs. The implementation flowchart of four kinds of control modes is given in Fig.5.

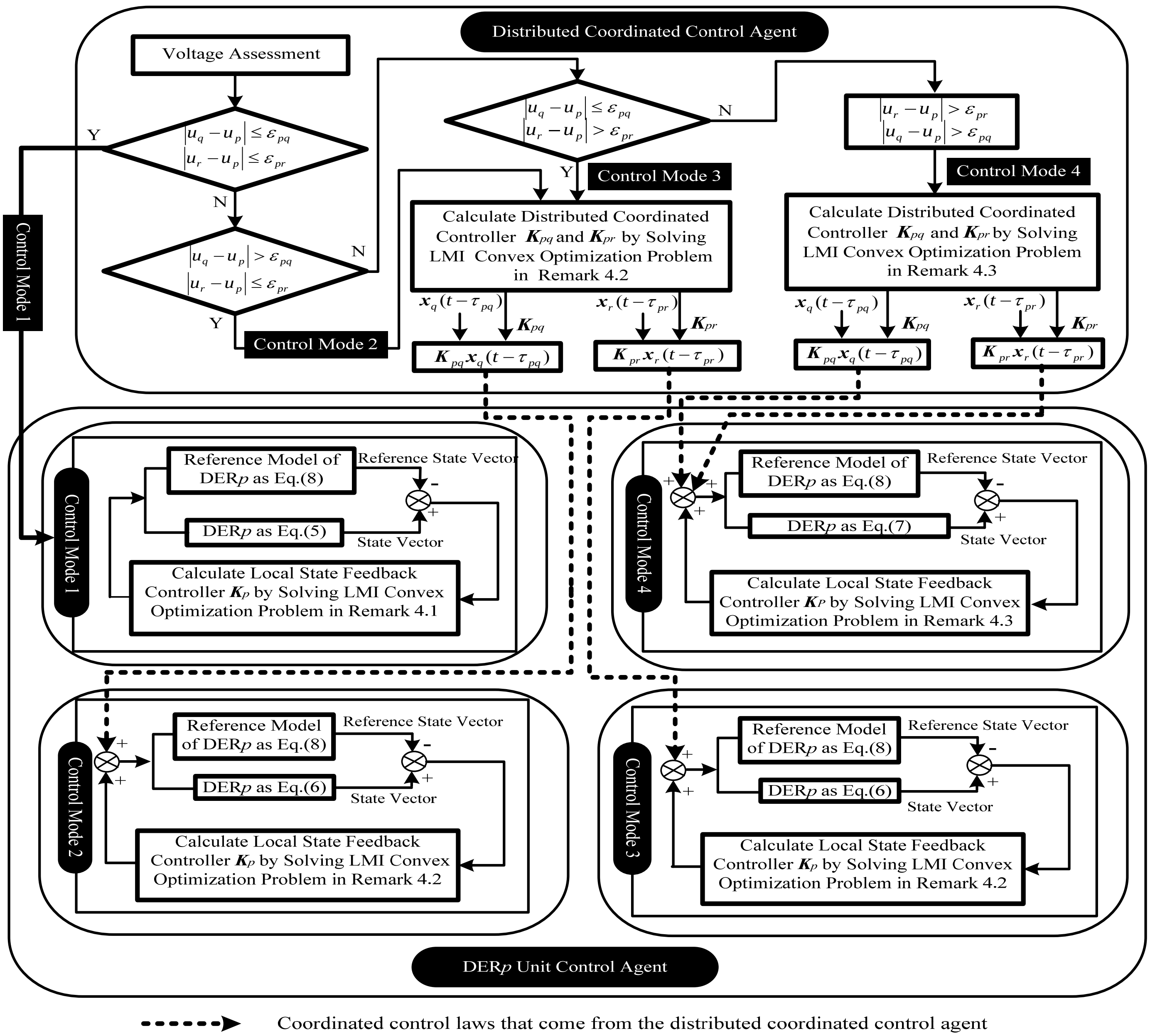

Fig.5 Implementation flowchart of four kinds of control modes based on the MAS

V. Experiment Studies

To evaluate the performance of the distributed coordinated control in a radial DC MG, two kinds of cases are designed in order to test different scenarios. The two cases mainly focus on two aspects: the control performance in response to different load changes, as well as the control performance in different time delays. The simulation parameters are given in Table.1.

Table 1. Simulation parameters

Parameter	Symbol	Value
DC power supply	U_{DC}	1kV
Output capacitance	C_p	2.2mF
Output capacitance	C_q	2.0mF
Output capacitance	C_r	1.8mF
Converter inductance	L_{tp}	2.0mH
Converter inductance	L_{tq}	1.8mH
Converter inductance	L_{tr}	1.6mH
Converter resistance	R_{tp}	0.2Ω
Converter resistance	R_{tq}	0.2Ω
Converter resistance	R_{tr}	0.2Ω
Transmission line inductance	L_{pq}	2.0 μH
Transmission line resistance	R_{pq}	0.05Ω
Transmission line inductance	L_{pr}	2.2 μH
Transmission line resistance	R_{pr}	0.06Ω

A. Case 1: the load demand doubled in the DERj

The load demand in the DERq increases twice at t=3s instant as shown in Fig.6(a). The load current disturbance leads to a big bus voltage deviation between both *pth* and *qth* DER units, i.e. $|u_q - u_p| > \varepsilon_{pq}$ and $|u_r - u_p| \le \varepsilon_{pr}$. In this case, the secondary-level agent determines to execute the distributed coordinated control mode 2 in both pth and qth DER units after t=3s, while the rth DER unit is still controlled by local control mode 1. By solving LMI convex optimization problem in Remark 4.2, we find that the integrated system of both pth and qth DER units is robust stable for any time delays satisfying $0 \le \bar{\tau} \le 2.2848s$. For the comparison purpose, in Figs.6(b) and (c), we firstly give the PCC voltage performance of both pth and qth DER units still in local control mode 1 after t=3s. Then the PCC voltage performance in the proposed distributed coordinated control mode 2 is displayed in Figs.6(d)-(g) taking into account different time delays.

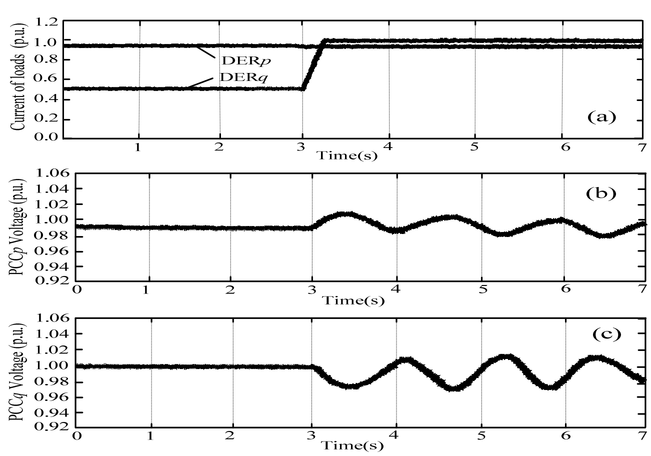

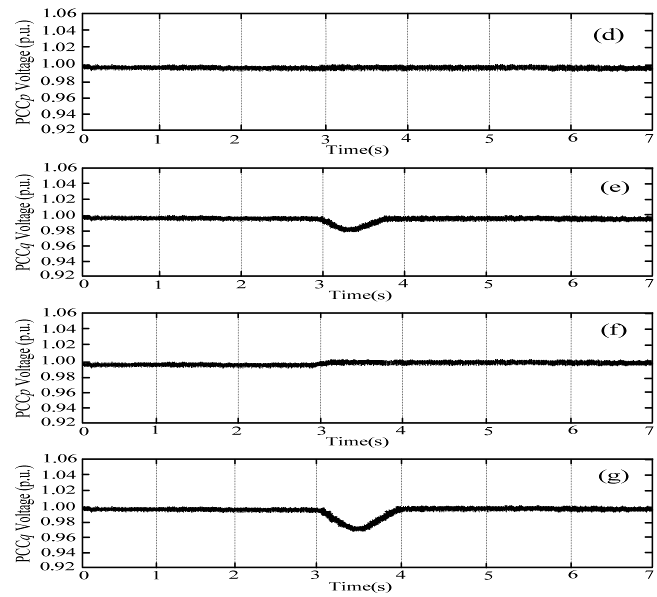

Fig.6 PCC control performance in Case 1

(a) Load currents in the DERp and DERq; (b) PCC voltage of the DERp in the local control mode 1 when τ=20ms; (c) PCC voltage of the DERq in the local control mode 1 when τ=20ms; (d) PCC voltage of the DERp in the distributed coordinated control mode 2 when τ=20ms; (e) PCC voltage of the DERq in the distributed coordinated control mode 2 when τ=20ms; (f) PCC voltage of the DERp in the distributed coordinated control mode 2 when τ=2s; (g) PCC voltage of the DERq in the distributed coordinated control mode 2 when τ=2s

From Figs.6(b) and (c), it can be shown that if the two DER units are still controlled by means of the local control mode 1 after t=3s, the PCC bus voltages, especially the PCCq voltage, have larger fluctuation. It is because that, only by local controller in each unit control agent, no decoupling control signal eliminates the coupling effect between both pth and qth DER units, so that the bus voltage deviation can not be controlled effectively. From Figs.6(d)-(g), it can be implied that, by means of the proposed distributed coordinated control mode 2, the PCC voltages of both pth and qth DER units can be stabilized within the secure range with less bus voltage deviation. Moreover, although taking into account different time delays, the PCC voltage performance in each DER is almost same. It is because that, by solving LMI convex optimization problem in Remark 4.2, as long as $\tau_{pq} \in [0, \bar{\tau}]$, the designed distributed coordinated controller can guarantee the system optimal control performance. The above simulation results imply that the MAS based distributed coordinated control can improve bus voltage performance in response to the load change and different transmission time delays.

Also for comparison purpose, Fig.7 gives the voltage performance by means of the proposed method of reference [12] in Case 1.

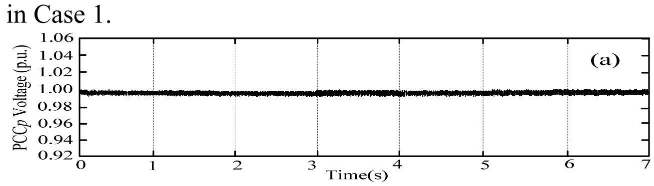

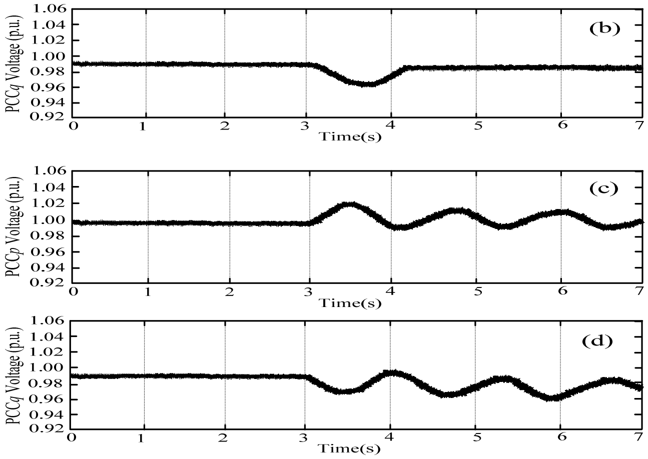

Fig.7 PCC control performance by means of the proposed method of reference [12] in Case 1

(a) PCC voltage of the DERp when τ=20ms; (b) PCC voltage of the DERq when τ=20ms; (c) PCC voltage of the DERp when τ=2s; (d) PCC voltage of the DERq when τ=2s

When τ=20ms, the voltage performance in Figs.7(a) and (b) by means of the proposed method of reference [12] is similar to that in Figs.6(d) and (e), only there is a bit larger deviation between both pth and qth bus voltages than in Figs.6(d) and (e). While when τ=2s, compared with Figs.6(f) and (g), there are larger voltage fluctuations in Figs.7(c) and (d) by means of the proposed method of reference [12] after t=3s. These voltage fluctuations can lead to much larger voltage deviation between both pth and qth DER units. The comparative results above imply that the proposed MAS based distributed coordinated control has better control performance especially in large time delays.

B. Case 2: the load changes in both DERp and DERq

The load demand in the DERq increases twice at t=3s instant, at the same time, the load demand in the DERp decreases half as shown in Fig.7(a). The load changes in the two DER units result in a larger bus voltage deviation among three adjacent DER units, i.e. $|u_q - u_p| > \varepsilon_{pq}$ and $|u_r - u_p| > \varepsilon_{pr}$. Therefore, the secondary-level agent determines to execute the distributed coordinated control mode 4 for the pth, qth and rth DER units after t=3s. By using LMI convex optimization technique in Remark 4.3, it can be found that the augmented system by integrating the pth, qth and rth DER units is asymptotically stable for any time delays satisfying $0 \le \bar{\tau} \le 2.1774s$. To evaluate the performance of the distributed coordinated control by comparison with the local control, the PCC voltage performance in the local control mode 1 is firstly given in Figs.7(b)-(d). Then taking into account different time delays, the PCC voltage performance in the distributed coordinated control mode 4 is displayed in Figs.7(e)-(j).

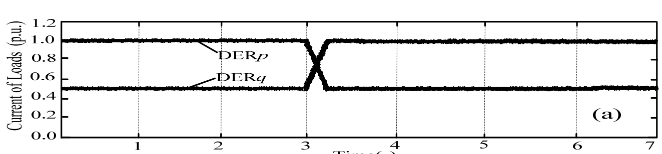

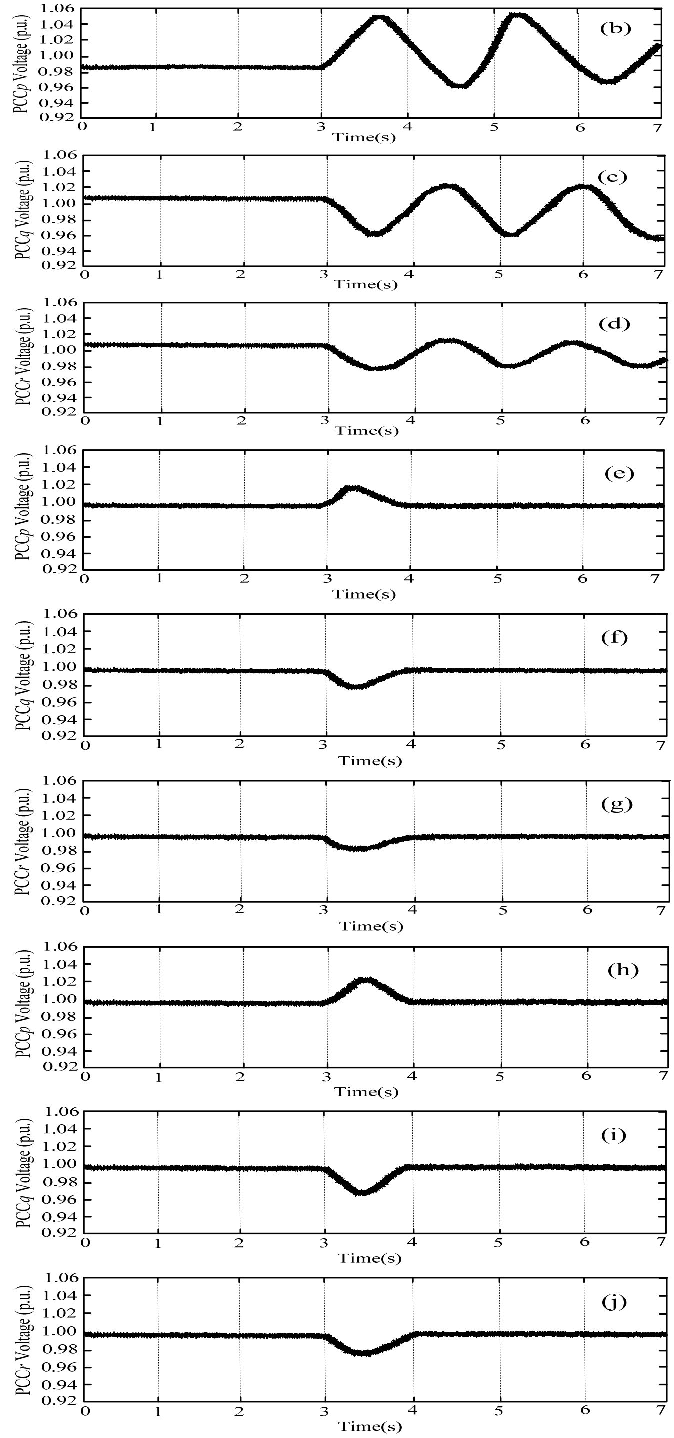

Fig.8 PCC voltage control performance in Case 2

(a) Load currents in the DERp and DERq; (b) PCC voltage of the DERp in the local control mode 1 when τ=200ms; (c) PCC voltage of the DERq in the local control mode 1 when τ=200ms; (d) PCC voltage of the DERr in the local control mode 1 when τ=200ms; (e) PCC voltage of the DERp in the distributed coordinated control mode 4 when τ=200ms; (f) PCC voltage of the DERq in the distributed coordinated control mode 4 when τ=200ms; (g) PCC voltage of the DERr in the distributed coordinated control mode 4 when τ=200ms; (h) PCC voltage of the DERp in the distributed coordinated control mode 4 when τ=2s; (i) PCC voltage of the DERq in the distributed coordinated control mode 4 when τ=2s; (i) PCC voltage of the DERr in the distributed coordinated control mode 4 when τ=2s

From Figs.8(b)-(d), it can seen that the local control is not able to maintain the PCC bus voltage stabilization in Case 2. There are very large voltage deviations especially between both *p*th and *q*th DER units since there are larger load changes in the two units. From Figs.8(e)-(j), it can shown that by means of the proposed distributed coordinated control mode 4, at the *t*=3s instant, the larger load disturbances only lead to a bit bus voltage fluctuations in the three DER units, afterwards the PCC voltages are rapidly stabilized down almost without any deviation in different time delays. The simulation results above indicate that the proposed MAS based distributed coordinated control still can ensure the bus voltages performance better in the face of larger load disturbances.

In order to testify the performance regarding current sharing by comparison with the proposed method of reference [12], the current performance is given in Fig.9 by using two kinds of methods taking into account different time delays in Case 2.

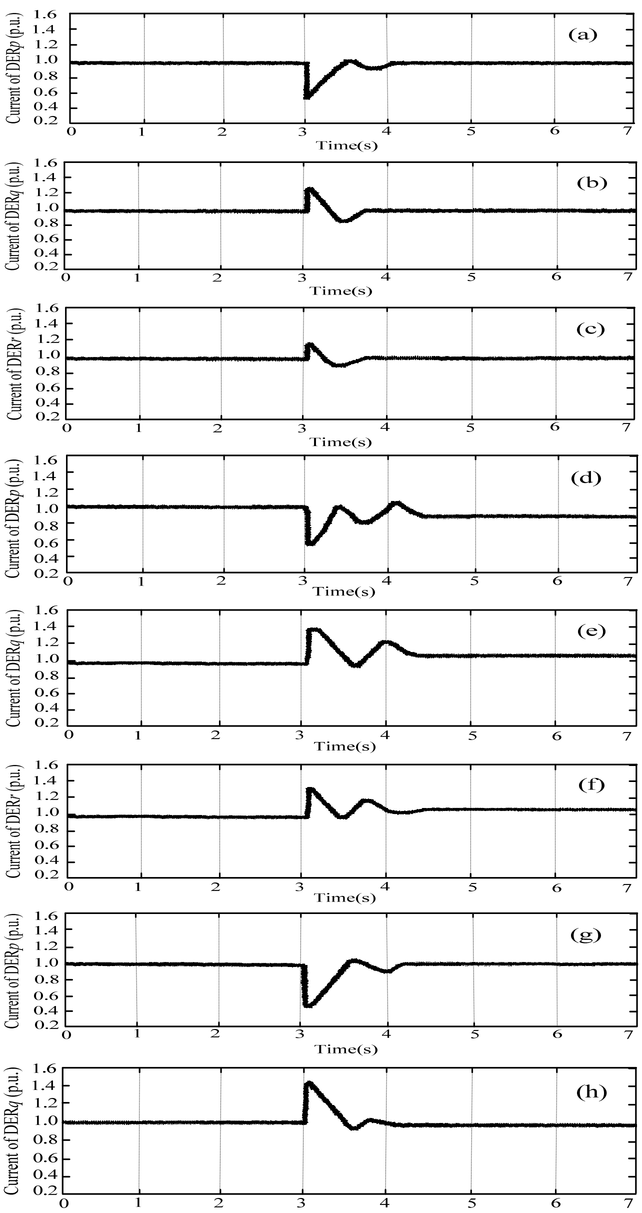

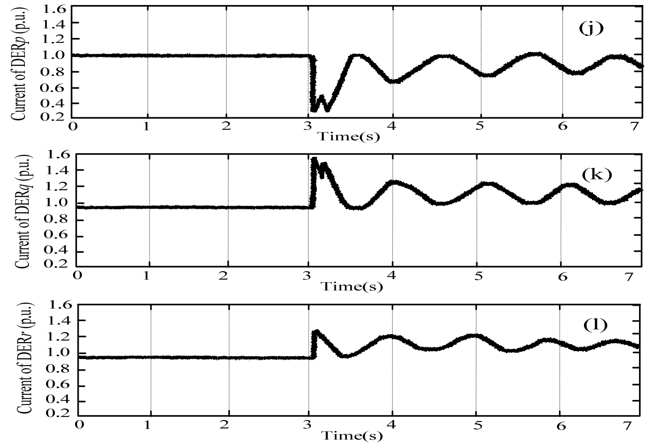

Fig.9 Current control performance in Case 2

(a) Current of the DER*p* in the proposed control mode 4 when τ=200ms; (b) Current of the DER*q* in the proposed control mode 4 when τ=200ms; (c) Current of the DER*r* in the proposed control mode 4 when τ=200ms; (d) Current of the DER*p* in the proposed method of reference [12] when τ=200ms; (e) Current of the DER*q* in the proposed method of reference [12] when τ=200ms; (f) Current of the DER*r* in the proposed method of reference [12] when τ=200ms; (g) Current of the DER*p* in the proposed control mode 4 when τ=2s; (h) Current of the DER*q* in the proposed control mode 4 when τ=2s; (i) Current of the DER*r* in the proposed control mode 4 when τ=2s; (j) Current of the DER*p* in the proposed method of reference [12] when τ=2s; (k) Current of the DER*q* in the proposed method of reference [12] when τ=2s; (l) Current of the DER*r* in the proposed method of reference [12] when τ=2s

From Figs.9(a)-(f), it can be shown that when τ=200ms, the current sharing in the three DER units by means of the proposed control mode 4 is a bit better than that in the proposed method of reference [12], since after *t*=4.5s there are a bit current deviation among the three DER units by means of the proposed method of reference [12]. When τ=2s, the current sharing is almost similar to that when τ=200ms in the each DER unit by means of the proposed control mode 4 as shown in Figs.(g)-(i). While by means of the proposed method of reference [12], when τ=2s, after *t*=3s there are very large current fluctuations in the three DER units, which leads to much larger current sharing deviation among the three DER units. The results above imply that when there is a large time delay, the proposed method in this paper can achieve better performance regarding current sharing.

In order to illustrate the robust performance of the proposed method, we assume that there is a failure of the communication link between both *p*th and *q*th secondary-level agents. Still in Case 2, the voltage performance of the three DER units is shown in Fig.10.

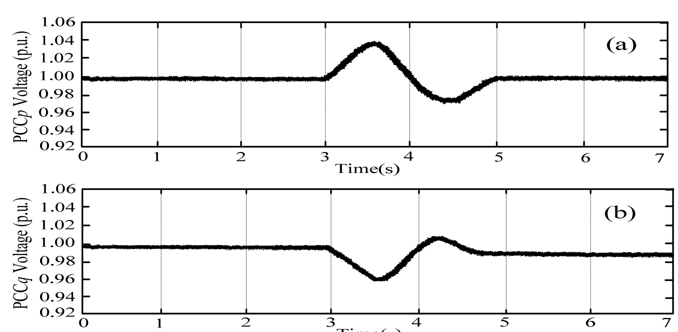

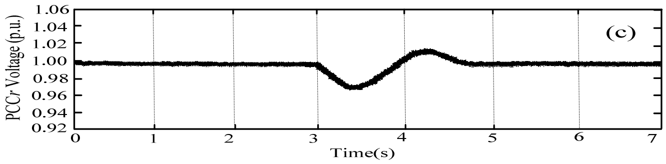

Fig.10 Voltage control performance when there is a failure of the communication in Case 2 when τ =200ms

(a) PCC voltage of the DER*p*; (b) PCC voltage of the DER*q*; (c) PCC voltage of the DER*r*

If there is no failure of the communication link between both *p*th and *q*th secondary-level agents, in case 2 the voltage performance in the three DER units should be the same as Figs.8(e)-(g). Therefore, compared with Figs.8(e)-(g), the PCC voltage fluctuations in the three DER units as shown in Figs.10(a)-(c) are a bit larger. However, the voltage fluctuations can damp down after *t*=4.5s. it is because that, though there is a failure of the communication link between both *p*th and *q*th secondary-level agents, but based on the MAS platform, through the interactions between first-level and secondary-level agents of *p*th DER unit and of *q*th DER units, as well as the interaction between both *p*th and *q*th first-level agents, the coordinated control laws between both *p*th and *q*th DER units can be still sent. Therefore, the proposed MAS distributed coordinated control method still can guarantee the PCC voltage stabilization. Only since it takes a larger time when the coordinated control laws are sent than that without failure, PCC voltage fluctuations are a bit larger.

VI. Conclusion

This paper develops a delay-dependent distributed coordinated control based on the two-level MAS, so that the DC MG can ensure voltage and current sharing performance better in response to large load disturbances and different time delays. Compared with the relevant research results, this paper contributes the following original works: The MAS based distributed coordinated control is proposed, where beside local-state-feedback control in unit control agent, the remote states that only come from adjacent DER based on low bandwidth communication are used to synthesize decoupling coordinated control law by means of the distributed coordinated control agent. Moreover, taking into account transmission time delays, the distributed coordinated control is designed by means of delay-dependent H_∞ robust control method. Finally, the better control performance has been demonstrated by means of simulation results.

However, the MAS based distributed coordinated control scheme still a bit relies on communication technology. Based on communication technology, the scheme can not only be applied into DC MG, but also be feasible for controlling any kind of smart grids with multiple DERs by extending the control function of the agents and creating additional agents in the system. The future development of this study will focus on extending application.

Acknowledgment

This work is supported by the National Natural Science Foundation of China under Grant 61573300, 61533010, 61403209 & 613040439.

Appendix A. Proof of Theorem 4.1:

Define a Lyapunov function for the tracking system (10) as

$$\mathrm{V}_i(t) = \hat{\boldsymbol{x}}_i^T(t)\boldsymbol{P}_i\hat{\boldsymbol{x}}_i(t), \text{ where } \boldsymbol{P}_i = \boldsymbol{P}_i^T > 0.$$

Then, it is easy to obtain

$$\int_0^{t_f}[(\boldsymbol{x}_i(t)-\boldsymbol{x}_{ri}(t))^T\boldsymbol{Q}_i(\boldsymbol{x}_i(t)-\boldsymbol{x}_{ri}(t))]dt = \int_0^{t_f}\hat{\boldsymbol{x}}_i^T(t)\hat{\boldsymbol{Q}}_i\hat{\boldsymbol{x}}_i(t)dt$$

$$= \hat{\boldsymbol{x}}_i^T(0)\boldsymbol{P}_i\hat{\boldsymbol{x}}_i(0) - \hat{\boldsymbol{x}}_i^T(t_f)\boldsymbol{P}_i\hat{\boldsymbol{x}}_i(t_f)$$

$$+\int_0^{t_f}\{\hat{\boldsymbol{x}}_i^T(t)\hat{\boldsymbol{Q}}_i\hat{\boldsymbol{x}}_i(t) + \frac{d}{dt}(\hat{\boldsymbol{x}}_i^T(t)\boldsymbol{P}_i\hat{\boldsymbol{x}}_i(t))\}dt$$

$$\le \hat{\boldsymbol{x}}_i^T(0)\boldsymbol{P}_i\hat{\boldsymbol{x}}_i(0) + \int_0^{t_f}\{\hat{\boldsymbol{x}}_i^T(t)\hat{\boldsymbol{Q}}_i\hat{\boldsymbol{x}}_i(t) + \dot{\hat{\boldsymbol{x}}}_i^T(t)\boldsymbol{P}_i\hat{\boldsymbol{x}}_i(t) + \hat{\boldsymbol{x}}_i^T(t)\boldsymbol{P}_i\dot{\hat{\boldsymbol{x}}}_i(t)\}dt$$

$$= \hat{\boldsymbol{x}}_i^T(0)\boldsymbol{P}_i\hat{\boldsymbol{x}}_i(0) + \int_0^{t_f}\left\{\begin{bmatrix}\hat{\boldsymbol{x}}_i(t)\\ \hat{\boldsymbol{\omega}}_i(t)\end{bmatrix}^T\begin{bmatrix}\hat{\boldsymbol{A}}_i^T\boldsymbol{P}_i + \boldsymbol{P}_i\hat{\boldsymbol{A}}_i + \hat{\boldsymbol{Q}}_i & \boldsymbol{P}_i\hat{\boldsymbol{D}}_i\\ \hat{\boldsymbol{D}}_i^T\boldsymbol{P}_i & -\rho_i^2\boldsymbol{I}\end{bmatrix}\begin{bmatrix}\hat{\boldsymbol{x}}_i(t)\\ \hat{\boldsymbol{\omega}}_i(t)\end{bmatrix}\right.$$

$$\left. + \rho_i^2\hat{\boldsymbol{\omega}}_i(t)^T\hat{\boldsymbol{\omega}}_i(t)\right\}dt$$

By the above inequality, it can be implied that if the inequality (13) is satisfied, the *i*th augmented DER unit system (10) is asymptotically stable with the guaranteed H_∞ control performance in (12) for $\forall\hat{\boldsymbol{\omega}}_i(t)$. The proof is completed.

Appendix B. Proof of Theorem 4.2

In order to prove the Theorem 4.2, firstly give a Lemma.

***Lemma 1[21]*:** For all vectors **a** and **b**, matrices $\boldsymbol{N}$、$\boldsymbol{X}$、$\boldsymbol{Y}$、$\boldsymbol{Z}$ with appropriate dimensions，if $\begin{bmatrix}\boldsymbol{X} & \boldsymbol{Y}\\ \boldsymbol{Y}^T & \boldsymbol{Z}\end{bmatrix} \ge 0$, then

$$-2\boldsymbol{a}^T\boldsymbol{N}\boldsymbol{b} \le \inf_{X,Y,Z}\left\{\begin{bmatrix}\boldsymbol{a}\\ \boldsymbol{b}\end{bmatrix}^T\begin{bmatrix}\boldsymbol{X} & \boldsymbol{Y}-\boldsymbol{N}\\ \boldsymbol{Y}^T-\boldsymbol{N}^T & \boldsymbol{Z}\end{bmatrix}\begin{bmatrix}\boldsymbol{a}\\ \boldsymbol{b}\end{bmatrix}\right\},$$

where, $\boldsymbol{X}$ and $\boldsymbol{Z}$ are symmetrical positive matrices.

Define a delay-dependent Lyapunov function for the system (18) as

$$\mathrm{V}(t) = \mathrm{V}_1(t) + \mathrm{V}_2(t) + \mathrm{V}_3(t) \tag{1B}$$

where $\mathrm{V}_1(t) = \tilde{\boldsymbol{x}}^T(t)\boldsymbol{P}\tilde{\boldsymbol{x}}(t)$, $\mathrm{V}_2(t) = \int_{t-\bar{\tau}}^{t}\tilde{\boldsymbol{x}}^T(\tau)\boldsymbol{S}\tilde{\boldsymbol{x}}(\tau)d\tau$,

$$\mathrm{V}_3(t) = \int_{-\bar{\tau}}^{0}\int_{t+\beta}^{t}\dot{\tilde{\boldsymbol{x}}}^T(\alpha)\boldsymbol{Z}\dot{\tilde{\boldsymbol{x}}}(\alpha)d\alpha d\beta.$$

And $\boldsymbol{P}$, $\boldsymbol{S}$, $\boldsymbol{Z}$ are symmetric positive definite weighting matrices.

The derivative of $\mathrm{V}_1(t)$ along the trajectory of system (18) satisfies that

$$\dot{\mathrm{V}}_{i1}(t) = 2\tilde{\boldsymbol{x}}^T(t)\boldsymbol{P}\ (\tilde{\boldsymbol{A}} + \widehat{\boldsymbol{A}})\ \bar{\boldsymbol{x}}_i(t) - 2\tilde{\boldsymbol{x}}^T(t)\boldsymbol{P}\widehat{\boldsymbol{A}}\int_{t-\bar{\tau}}^{t}\dot{\tilde{\boldsymbol{x}}}(\alpha)d\alpha + 2\tilde{\boldsymbol{x}}^T(t)\boldsymbol{P}\tilde{\boldsymbol{D}}\tilde{\boldsymbol{\omega}}(t)$$

By using Lemma 3.1, it is very easy to obtain

$$-2\tilde{\boldsymbol{x}}^T(t)\boldsymbol{P}\widehat{\boldsymbol{A}}\dot{\tilde{\boldsymbol{x}}}(\alpha) \le \tilde{\boldsymbol{x}}^T(t)\boldsymbol{X}\tilde{\boldsymbol{x}}(t)$$

$$+\dot{\tilde{\boldsymbol{x}}}^T(\alpha)[\boldsymbol{Y}^T - (\boldsymbol{P}\widehat{\boldsymbol{A}})^T]\tilde{\boldsymbol{x}}(t) + \tilde{\boldsymbol{x}}^T(t)(\boldsymbol{Y} - \boldsymbol{P}\widehat{\boldsymbol{A}})\dot{\tilde{\boldsymbol{x}}}(\alpha) + \dot{\tilde{\boldsymbol{x}}}^T(\alpha)\boldsymbol{Z}\dot{\tilde{\boldsymbol{x}}}(\alpha)$$

Then $\dot{\mathrm{V}}_1(t) \le \{\tilde{\boldsymbol{x}}^T(t)(\boldsymbol{P}\tilde{\boldsymbol{A}} + \tilde{\boldsymbol{A}}^T\boldsymbol{P} + \bar{\tau}\boldsymbol{X} + \boldsymbol{Y} + \boldsymbol{Y}^T\}\tilde{\boldsymbol{x}}(t)$

$$-2\tilde{\boldsymbol{x}}^T(t)(\boldsymbol{Y} - \boldsymbol{P}\widehat{\boldsymbol{A}})\tilde{\boldsymbol{x}}(t-\bar{\tau}) + \int_{t-\bar{\tau}}^{t}\dot{\tilde{\boldsymbol{x}}}^T(\alpha)\boldsymbol{Z}\dot{\tilde{\boldsymbol{x}}}(\alpha)d\alpha + 2\tilde{\boldsymbol{x}}^T(t)\boldsymbol{P}\tilde{\boldsymbol{D}}\tilde{\boldsymbol{\omega}}(t)\}\cdot \tag{2B}$$

The derivative of other Lyapunov functions along the trajectory of system (18) satisfy that

$$\dot{\mathrm{V}}_2(t) = \tilde{\boldsymbol{x}}^T(t)\boldsymbol{S}\tilde{\boldsymbol{x}}(t) - \tilde{\boldsymbol{x}}^T(t-\bar{\tau})\boldsymbol{S}\tilde{\boldsymbol{x}}(t-\bar{\tau}) \tag{3B}$$

$$\dot{\mathrm{V}}_3(t) = \bar{\tau}\dot{\tilde{\boldsymbol{x}}}^T(t)\boldsymbol{Z}\dot{\tilde{\boldsymbol{x}}}(t) - \int_{t-\bar{\tau}}^{t}\dot{\tilde{\boldsymbol{x}}}^T(\alpha)\boldsymbol{Z}\dot{\tilde{\boldsymbol{x}}}(\alpha)d\alpha \tag{4B}$$

Then, it can be obtained

$$\int_0^{t_f}\tilde{\boldsymbol{x}}^T(t)\tilde{\boldsymbol{Q}}\tilde{\boldsymbol{x}}(t)dt = \mathrm{V}(0) - \mathrm{V}(t_f) + \int_0^{t_f}\{\tilde{\boldsymbol{x}}^T(t)\tilde{\boldsymbol{Q}}\tilde{\boldsymbol{x}}(t) + \dot{\mathrm{V}}(t)\}dt$$

$$\le \mathrm{V}(0) + \int_0^{t_f}\{\tilde{\boldsymbol{x}}^T(t)(\tilde{\boldsymbol{Q}} + \boldsymbol{S} + \boldsymbol{P}\tilde{\boldsymbol{A}} + \tilde{\boldsymbol{A}}^T\boldsymbol{P} + \bar{\tau}\boldsymbol{X} + \boldsymbol{Y} + \boldsymbol{Y}^T)\tilde{\boldsymbol{x}}(t)$$

$$-2\tilde{\boldsymbol{x}}^T(t)(\boldsymbol{Y}-\boldsymbol{P}\hat{\boldsymbol{A}})\tilde{\boldsymbol{x}}(t-\bar{\tau})+2\tilde{\boldsymbol{x}}^T(t)\boldsymbol{P}\tilde{\boldsymbol{D}}\tilde{\boldsymbol{\omega}}(t)-\tilde{\boldsymbol{x}}^T(t-\bar{\tau})\boldsymbol{S}\tilde{\boldsymbol{x}}(t-\bar{\tau})$$

$$+\bar{\tau}\dot{\tilde{\boldsymbol{x}}}^T(t)\boldsymbol{Z}\dot{\tilde{\boldsymbol{x}}}(t)+\rho^2\tilde{\boldsymbol{\omega}}^T(t)\tilde{\boldsymbol{\omega}}(t)-\rho^2\tilde{\boldsymbol{\omega}}^T(t)\tilde{\boldsymbol{\omega}}(t)\}dt$$

$$=\mathrm{V}(0)+\int_0^{t_f}\left\{\begin{bmatrix}\tilde{\boldsymbol{x}}(t)\\ \tilde{\boldsymbol{x}}(t-\bar{\tau})\\ \tilde{\boldsymbol{\omega}}(t)\end{bmatrix}^T\left\{\begin{bmatrix}\Theta & \boldsymbol{P}\hat{\boldsymbol{A}}-\boldsymbol{Y} & \boldsymbol{P}\tilde{\boldsymbol{D}}\\ * & -\boldsymbol{S} & 0\\ * & * & -\rho^2\end{bmatrix}\right.\right.$$

$$\left.+\bar{\tau}\begin{bmatrix}\tilde{\boldsymbol{A}}\\ \hat{\boldsymbol{A}}\\ \tilde{\boldsymbol{D}}\end{bmatrix}^T\boldsymbol{Z}\begin{bmatrix}\tilde{\boldsymbol{A}}\\ \hat{\boldsymbol{A}}\\ \tilde{\boldsymbol{D}}\end{bmatrix}\right\}\begin{bmatrix}\tilde{\boldsymbol{x}}(t)\\ \tilde{\boldsymbol{x}}(t-\bar{\tau})\\ \tilde{\boldsymbol{\omega}}(t)\end{bmatrix}+\rho^2\tilde{\boldsymbol{\omega}}^T(t)\tilde{\boldsymbol{\omega}}(t)\}dt$$

According to the above inequality, by using Schur complement, it is easy to obtain that, if the inequality (20) hold, the system (18) is asymptotically stable with the H_∞ performance in (19). This completes the proof.

References

[1] A. Kwasinski, "Quantitative evaluation of dc microgrids availability: Effects of system architecture and converter topology design choices," *IEEE Trans on Power Electronics*, vol. 26, no. 3, pp. 835–851, 2011.

[2] Q. Shafiee, T. Dragi˘cevi´c, J. C. Vasquez, and J. M. Guerrero, "Hierarchical Control for Multiple DC-Microgrids Clusters," *IEEE Trans on Energy Conversion*, vol. 29, no. 4, pp. 922–933, 2014.

[3] A. T. Elsayed, A. A. Mohamed, and O. A. Mohammed, "DC microgrids and distribution systems: An overview," *Electric Power Systems Research*, vol. 119, pp. 407–417, 2015.

[4] W. Yao, M. Chen, J. Matas, J. M. Guerrero, Z. M. Qian, "Design and analysis of the droop control method for parallel inverters considering the impact of the complex impedance on the power sharing," *IEEE Trans on Industrial Electronics*, vol. 58, no. 2, pp. 576-588, 2011.

[5] A. Khorsandi, M. Ashourloo, H. Mokhtari, "A Decentralized control method for a low-voltage DC Microgrid," *IEEE Trans on Energy Conversion*, vol. 29, no. 4, pp. 793–801, 2014.

[6] Y. J Gu, X. Xiang, W. H. Li , X. N. He, "Mode-adaptive decentralized control for renewable DC Microgrid with enhanced reliability and flexibility," *IEEE Trans on Power Electronics*, vol. 29, no. 9, pp. 5072-5080, 2013.

[7] J. M. Guerrero, J. C. Vasquez, J. Matas, J. G. Vicuna, M. Castilla," Hierarchical control of droop-controlled AC and DC microgrids—a general approach toward standardization." *IEEE Trans on Industrial Electronics*, vol. 58, no. 1, pp. 158-172, 2011.

[8] X. Lu, J. M. Guerrero, K. Sun, J. C. Vasquez, R. Teodorescu, L. Huang, "Hierarchical control of parallel ac-dc converter interfaces for hybrid microgrids," *IEEE Trans Smart Grid*, vol. 5, no. 2, pp. 683-692, 2014.

[9] A. Bidram, and A. Davoudi, "Hierarchical structure of microgrids control system," *IEEE Trans. Smart Grid*, vol. 3, no. 4, pp. 1963-1976, 2012.

[10] M. Guerrero, L. P. Chiang, T. L. Lee, M. Chandorkar, "Advanced control architectures for intelligent Microgrids—Part II : Power quality, energy storage, and AC/DC Microgrids," *IEEE Trans on Industrial Electronics*, vol. 60, no.4, pp. 1263-1270, 2013.

[11] Q. Shafiee, J. M. Guerrero, J. C. Vasquez, "Distributed secondary control for islanded MicroGrids - A novel approach," *IEEE Trans on Power Electronics*, vol. 29, no.2, pp. 1018-1031, 2014.

[12] S. Anand, B. G. Fernandes, and J. M. Guerrero, "Distributed control to ensure proportional load sharing and improve voltage regulation in low-voltage dc microgrids," IEEE Trans. Power Electron., vol. 28, no. 4, pp. 1900-1913, 2013.

[13] X. Lu, J. M. Guerrero, K. Sun, and J. C. Vasquez, "An improved droop control method for dc microgrids based on low bandwidth communication with dc bus voltage restoration and enhanced current sharing accuracy," IEEE Trans. Power Electron., vol. 29, no. 4, pp. 1800-1812, 2014

[14] Q Shafiee, C. Stefanovic, T. Draginevic, P. Popovskii, J. Vasquez, J. M. Guerrero, "Robust network control scheme for distributed secondary control of islanded Mirogrid," *IEEE Trans on Industrial Electronics*, vol. 60, no.10, pp. 5363-5374, 2014.

[15] A. Bidram, A. Davoudi, F. L. Lwis, and J. M. Guerrero, "Distributed cooperative secondary control of microgrids using feedback linearization," *IEEE Trans Power System*, vol. 28, no. 3, pp. 3462-3470, 2013.

[16] V. Nasirian, S. Moayedi, A. Davoudi, F. L. Lewis, "Distributed cooperative control for DC Microgrid," *IEEE Trans on Power Electronics*, vol. 30, no.4, pp. 2288–2303, 2015.

[17] S. Moayedi, A. Davoudi, F. L. Lewis, "Distributed adaptive droop control for DC distributed system," *IEEE Trans on Energy Conversion*, vol. 29, no. 4, pp. 944–956, 2014.

[18] C. Balarko, M. Rajat, C. P. Bikash, "Wide-area measurement- based stabilizing control of power system considering signal transmission delay," *IEEE Trans on power system*, vol.19, no. 4, pp. 1971-1979, 2004.

[19] H. X Wu, K. S. Taakalis, G. T Heydt, "Evaluation of time delay effects to wide-area power system stabilizer design," *IEEE Trans. on power system*, vol.19, no 4, pp. 1935-1941, 2004.

[20] C. X. Dou, Q. Q. Jia, S. J. Jin, Z. Q. Bo, "Delay-independent decentralized stabilizer design for large interconnected power systems based on WAMS," *International Journal of Electrical Power & Energy Systems*, vol. 29, pp. 775-782, 2007.

[21] C.X. Dou, Z. S. Duan, X. B. Jia, "Delay-dependent H∞ robust control for large power systems based on two-level hierarchical decentralized coordinated control structure," *International Journal of Systems Science*, vol.42, no.1, pp. 201-217, 2013.

[22] T. Logenthiran, D. Srinivasan and A. M. Khambadkone, "Multi-agent system for energy resource scheduling of integrated microgrids in a distributed system," *Electric Power System Research,* vol. 81, no. 1, pp. 138-148, 2011.

[23] J. Lagorse, D. Paire, A. Miraoui, "A multi-agent system for energy management of distributed power sources," *Renewable Energy*, vol. 35, pp. 174-182, 2010.

[24] C. X. Dou, B. Liu, J. M. Guerrero, "Event-triggered hybrid control based on multi-agent system for microgrids," *IET Generation, Transmission & Distribution*, vol.12, pp.1987-1997, 2014.

[25] S. Riverso, F. Sarzo, G. Ferrari-Trecate, "Plug-and-play voltage and frequency control of islanded microgrids with meshed topology," *IEEE Trans on Smart Grid*, vol.6, no.3, pp.1176-1184, 2014.

Chunxia Dou received the B.S. and M.S. degrees in automation from the Northeast Heavy Machinery Institute, Qiqihaer, China, in 1989 and 1994, respectively, and the Ph.D. degree in Institute of Electrical Engineering from Yanshan University, Qinhuangdao, China, in 2005. In 2010, he joined the Department of Engineering, Peking University, Beijing, China, where he was a Postdoctoral Fellow for two years. Since 2005, she has been a Professor in Institute of Electrical Engineering, Yanshan University. Her current research interests include multi-agent based control, event-triggered hybrid control, distributed coordinated control, and multi-mode switching control and their applications in power systems, Microgrids and smart grids.

Dong Yue (SM'08) received the Ph.D. degree from the South China University of Technology, Guangzhou, China, in 1995. He is currently a professor and dean of Institute of Advanced Technology, Nanjing University of Posts and Telecommunications and also a Changjiang Professor with the Department of Control Science and Engineering, Huazhong University of Science and Technology. He is currently an Associate Editor of the IEEE Control Systems Society Conference Editorial Board and also an Associate Editor of the IEEE Transactions on Neural Networks and Learning Systems, the Journal of the Franklin Institute and the International Journal of Systems Science. Up to now, he has published more than 100 papers in international journals, domestic journals, and international conferences. His research interests include analysis and synthesis of networked control systems, multi-agent systems, optimal control of power systems, and internet of things.

Josep M. Guerrero (S'01-M'04-SM'08-FM'15) received the B.S. degree in telecommunications engineering, the M.S. degree in electronics engineering, and the Ph.D. degree in power electronics from the Technical University of Catalonia, Barcelona, in 1997, 2000 and 2003, respectively. Since 2011, he has been a Full Professor with the Department of Energy Technology, Aalborg University, Denmark, where he is responsible for the Microgrid Research Program. From 2012 he is a guest Professor at the Chinese Academy of Science and the Nanjing University of Aeronautics and Astronautics; from 2014 he is chair Professor in Shandong University; and from 2015 he is a distinguished guest Professor in Hunan University.

His research interests is oriented to different microgrid aspects, including power electronics, distributed energy-storage systems, hierarchical and cooperative control, energy management systems, and optimization of microgrids and islanded minigrids; recently specially focused on maritime microgrids for electrical ships, vessels, ferries and seaports. Prof. Guerrero is an Associate Editor for the IEEE TRANSACTIONS ON POWER ELECTRONICS, the IEEE TRANSACTIONS ON INDUSTRIAL ELECTRONICS, and the IEEE Industrial Electronics Magazine, and an Editor for the IEEE TRANSACTIONS on SMART GRID and IEEE TRANSACTIONS on ENERGY CONVERSION. He has been Guest Editor of the IEEE TRANSACTIONS ON POWER ELECTRONICS Special Issues: Power Electronics for Wind Energy Conversion and Power Electronics for Microgrids; the IEEE TRANSACTIONS ON INDUSTRIAL ELECTRONICS Special Sections: Uninterruptible Power Supplies systems, Renewable Energy Systems, Distributed Generation and Microgrids, and Industrial Applications and Implementation Issues of the Kalman Filter; and the IEEE TRANSACTIONS on SMART GRID Special Issue on Smart DC Distribution Systems. He was the chair of the Renewable Energy Systems Technical Committee of the IEEE Industrial Electronics Society. He received the best paper award of the IEEE Transactions on Energy Conversion for the period 2014-2015. In 2014 and 2015 he was awarded by Thomson Reuters as Highly Cited Researcher, and in 2015 he was elevated as IEEE Fellow for his contributions on “distributed power systems and microgrids.”

butions on “distributed power systems and microgrids.”

Xiangpeng Xie received the B.S. degree and Ph.D. degree in engineering from Northeastern University, Shenyang, China, in 2004 and 2010, respectively. From 2012 to 2014, he was a Postdoctoral Fellow with the Department of Control Science and Engineering, Huazhong University of Science and Technology. He is currently an Associate Professor with the Institute of Advanced Technology, Nanjing University of Posts and Telecommunications, Nanjing, China. His research interests include fuzzy modeling and control synthesis, state estimations, optimization in process industries and intelligent optimization algorithm

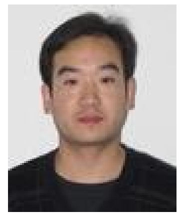

Song-Lin Hu received his Ph.D. degree in Department of Control Science and Engineering at Huazhong University of Science and Technology in 2012. He is currently an Associate Professor at the Institute of Advanced Technology, Nanjing University of Posts and Telecommunications. His research interests include networked control systems, event/self-triggered control, T-S fuzzy systems and time delay systems